JOURNAL OF VIROLOGY, Oct. 1999, p. 8762–8770 Vol. 73, No. 10
0022-538X/99/$04.00+0

Possible Interactions between the NS-1 Protein and Tumor Necrosis Factor Alpha Pathways in Erythroid Cell Apoptosis Induced by Human Parvovirus B19

N. SOL,[1] J. LE JUNTER,[1] I. VASSIAS,[1] J. M. FREYSSINIER,[2] A. THOMAS,[3] A. F. PRIGENT,[4] B. B. RUDKIN,[3] S. FICHELSON,[2] AND F. MORINET[1]*

Hôpital Saint-Louis, Virologie and CNRS UPR 9051,[1] and Hôpital Cochin, Laboratoire de Recherche en Hémobiologie,[2] Paris, Ecole Normale Superieure, CNRS UMR 49 Lyon,[3] and INSA-Lyon, INSERM U352, Villeurbanne,[4] France

Received 26 March 1999/Accepted 30 June 1999

Human erythroid progenitor cells are the main target cells of the human parvovirus B19 (B19), and B19 infection induces a transient erythroid aplastic crisis. Several authors have reported that the nonstructural protein 1 (NS-1) encoded by this virus has a cytotoxic effect, but the underlying mechanism of NS-1-induced primary erythroid cell death is still not clear. In human erythroid progenitor cells, we investigated the molecular mechanisms leading to apoptosis after natural infection of these cells by the B19 virus. The cytotoxicity of NS-1 was concomitantly evaluated in transfected erythroid cells. B19 infection and NS-1 expression induced DNA fragmentation characteristic of apoptosis, and the commitment of erythroid cells to undergo apoptosis was combined with their accumulation in the G_2 phase of the cell cycle. Since B19- and NS-1-induced apoptosis was inhibited by caspase 3, 6, and 8 inhibitors, and substantial caspase 3, 6, and 8 activities were induced by NS-1 expression, there may have been interactions between NS-1 and the apoptotic pathways of the death receptors tumor necrosis factor receptor 1 and Fas. Our results suggest that Fas-FasL interaction was not involved in NS-1- or B19-induced apoptosis in erythroid cells. In contrast, these cells were sensitized to tumor necrosis factor alpha (TNF-α)-induced apoptosis. Moreover, the ceramide level was enhanced by B19 infection and NS-1 expression. Therefore, our results suggest that there may be a connection between the respective apoptotic pathways activated by TNF-α and NS-1 in human erythroid cells.

The human parvovirus B19 (B19) infects the human erythroid progenitors, thereby reproducing the aplastic erythroblastopenic crisis observed upon in vivo infection (34). This crisis may also lead to chronic anemia, due to persistent infection of the immunocompromised host, and in utero infection can produce hydrops fetalis or congenital anemia (56). B19, which is small and nonenveloped, contains a linear single-stranded DNA genome, which encodes the two structural proteins VP-1 and VP-2 in its 3′ half and encodes the 77-kDa nonstructural protein 1 (NS-1) in its 5′ half (7). The NS-1 protein is involved in viral DNA replication and in the regulation of homologous and heterologous promoters (10, 30, 47). It has a nucleoside triphosphate-binding motif that supports ATPase and helicase enzymatic activities, which have been reported to be strongly linked to viral replication (6, 32).

Like many parvovirus nonstructural proteins, NS-1 of B19 is cytotoxic in vitro (23, 25, 40, 48), and its nucleoside triphosphate-binding domain appears to be involved in cytotoxicity (32). The existence of a link between toxicity and apoptosis in erythroid cell lines transfected to express the NS-1 gene has been suggested (31), and electron microscope studies of erythroblasts from B19-infected patients have revealed apoptotic features, including nucleolar degeneration, heterochromatin margination, and cytoplasmic vacuolation (33).

The apoptotic process can be induced by a variety of stimuli, leading to the activation of a specific series of metabolic and morphological changes, and by the activation of endogenous endonucleases that ultimately produce the typical DNA fragmentation at the internucleosomal level (reviewed in reference 14). There is increasing evidence that the apoptotic death process can be controlled by endogenous factors such as proto-oncogenes and by exogenous factors such as cytokines. CD95 (also called Fas) and tumor necrosis factor receptor 1 (TNFR1), the best-characterized death receptors, transmit apoptosis signals initiated by specific "death ligands" (reviewed in reference 2). These receptors are ubiquitously expressed in various tissues.

The binding of the Fas ligand (FasL) or tumor necrosis factor alpha (TNF-α) to its receptor induces the oligomerization of a homologous cytoplasmic sequence termed the "death domain," which combines with the death domains of other cellular proteins to stimulate apoptosis. The binding of FasL to Fas induces trimerization of the Fas receptor, which recruits caspase 8 (FLICE or MACH) via an adapter, the protein containing the Fas-associated death domain (FADD) (5). After TNF-induced trimerization of the receptor, the protein containing the receptor-associated death domain (TRADD) is recruited by the receptor death domain (17). TRADD functions as an adapter for the recruitment of several signaling molecules by the activated receptor. The TNFR-associated factor 2 (TRAF2) and the receptor-interacting protein stimulate pathways leading to the activation of nuclear factor kappa B (NF-κB), whereas FADD mediates the activation of apoptosis (16). NF-κB is a ubiquitously expressed transcription factor which was first found to be involved in the activation of genes associated with inflammation and subsequently in that of cell survival genes (3). An antiapoptotic function was recently described for NF-κB, and it was observed to be involved in resistance to cell death induced by TNF-α (4, 26). The central

* Corresponding author. Mailing address: Hôpital Saint-Louis, Virologie & UPR CNRS 9051, 1, avenue Claude Vellefaux, 75475 PARIS Cédex 10, France. Phone: 33 1 42 49 94 93. Fax: 33 1 42 49 92 00. E-mail: fr.morinet@chu-stlouis.fr.

component of apoptotic machinery is a proteolytic system involving a family of proteases called caspases (reviewed in reference 54). The interaction between caspase 8 and FADD appears to constitute a direct link between the signals in the membrane and the execution machinery (29). Caspase 8 is an initiator caspase which in turn activates effector caspases, and this results in cellular disassembly; caspase 8 is clearly associated with apoptosis involving death receptors, and inhibitors of caspase 3, an effector caspase, block Fas and TNFR1-induced apoptosis (12, 37, 52). An acidic sphingomyelinase might also be activated by FADD, thus generating ceramide (1, 45), which might induce apoptosis (18, 38), terminal differentiation, or cell cycle arrest in several cell types (15).

In the present work, we investigated the molecular mechanisms leading to erythroid cell death after natural infection by B19. This study was performed with purified normal human erythroid progenitors, and the cytotoxicity of NS-1 was evaluated concomitantly in a transfected erythroid cell line. Our findings indicate that B19 infection and NS-1 expression clearly induced apoptosis, and they suggest that there may be a connection between the respective apoptotic pathways activated by TNF-α and NS-1 in human erythroid cells.

MATERIALS AND METHODS

Primary erythroid cells and cell lines. Erythroid commitment of undifferentiated pluripotent stem cells provides early and late erythroid progenitors, the burst-forming-unit erythroid progenitors (BFU-E) and the colony-forming-unit erythroid progenitors (CFU-E), respectively. Purified normal human erythroid progenitors were obtained from serum-free cultures of $CD34^+$ cells from adult blood and cultured for 7 days with the combination of stem cell factor (SCF), interleukin 6 (IL-6), and IL-3. A large number of $CD36^+$ cells was thus obtained. The cells were isolated by immunomagnetic separation with a monoclonal CD36 immunoglobulin G1 (IgG1) antibody (Immunotech, Inc.) and a rat anti-mouse IgG1 antibody coupled to magnetic microbeads (Miltenyi Biotech). CD36 is a multifunctional glycoprotein receptor found early on erythroid progenitors, but it is a late marker of megakaryocytes and monocytes. The purified CD36 cells, which consisted of 96% late BFU-E and CFU-E, were again cultured in Iscove medium supplemented with 2 U of human recombinant erythropoietin (Epo; Boerhinger)/ml, 10 ng of IL-3/ml, 10 ng of IL-6/ml, and 25 ng of SCF (TEBU)/ml and left for 2 days (22).

The UT7 erythroleukemia cell line, which was adapted for growth by 6 months in Epo, has an erythroid differentiation (17). UT7 cells were propagated in α-modified Eagle's medium supplemented with 10% fetal calf serum, penicillin, streptomycin, 2 mM glutamine, and 2 U of Epo/ml.

The UT7 erythroleukemia cell line which stably expresses the NS-1 protein (UT7-NS) was established by cotransfection of the glucocorticoid receptor expression vector pCT-TK-GR-3.795 and the NS-1 expression vector pGRE5-2/EBV-NS. The *NS-1* gene was cloned under the control of a steroid-inducible promoter in the pGRE-2/EBV vector, which is episomal and contains the *Epstein Barr virus nuclear antigen-1* gene (24). A control cell line (UT7-pGRE) was also established by cotransfecting the glucocorticoid receptor expression vector and the empty vector pGRE5-2/EBV. The cells were mixed with 50 μg of plasmid DNA in 120 mM KCl, 15 mM $CaCl_2$, 10 mM K_2HPO_4-KH_2P0_4 (pH 7.6), 25 mM HEPES, 2 mM EGTA, 5 mM $MgCl_2$, 5 mM glutathione, 2 mM ATP and electroporated at 960 μF and 250 V (Gene Pulser; Bio-Rad). A stable cell line expressing NS-1 protein was obtained by hygromycin B selection (300 μg/ml) and induction with 10^{-6} M dexamethasone (DEX). NS-1 protein expression was then tested by immunofluorescence.

Human embryonic kidney 293 cells were propagated in Dulbecco's modified Eagle's medium supplemented with 10% fetal calf serum, penicillin, streptomycin, and 2 mM glutamine.

Erythroid cell infection. Sera containing B19 were obtained from patients with sickle cell disease and were found by dot blot analysis to contain 10^{12} copies of DNA per milliliter.

For infection, 10^7 CD36 cells were maintained in Iscove medium supplemented with 2 U of Epo/ml, 10 ng of IL-3/ml, 10 ng of IL-6/ml, and 25 ng of SCF/ml; inoculated with 40 μl of parvovirus-containing serum; left for 2 h at 4°C; and incubated for 1 h at 37°C. After extensive washing, the cells were diluted to 2×10^6/ml in Iscove medium supplemented with 2 U of Epo/ml, 10 ng of IL-3/ml, 10 ng of IL-6/ml, and 25 ng of SCF/ml.

Antibodies and reagents. Rabbit polyclonal antisera against NS-1, VP-1, and VP-2 were produced as previously described (41).

The goat polyclonal anti-human TNFR1 antibody C-20 (Santa Cruz Biotechnology) was used for immunofluorescence analysis. The purified anti-Fas monoclonal antibody agonist DX2 (PharMingen, San Diego, Calif.) and the purified anti-Fas monoclonal antibody antagonist ZB4 (Immunotech, Inc.) were added to infected and uninfected CD36 cells, and apoptosis was evaluated.

The predominant form of NF-κB exists in mammalian cells as a heterodimeric complex of 50- and 65-kDa protein subunits. For supershift experiments performed with the oligonucleotides containing NF-κB binding sites, p50 and p65 rabbit antibodies were kindly provided by N. Rice (Frederick Cancer Research and Development Center).

The cells were treated with the following caspase inhibitor peptides (50 μg/ml each): DEVD-CHO (Asp-Glu-Val-Asp aldehyde), an inhibitor of caspase 3 activity (Biomol, Plymouth Meeting, Pa.); IETD-CHO (Ile-Glu-Thr-Asp aldehyde), an inhibitor of caspase 6 and caspase 8 activities (Biomol); and zVAD-fmk (*Z*-Asp-Ala-Asp-fluoromethylketone), a broad-spectrum caspase inhibitor (Bachem).

C2-ceramide was provided by Biomol. Recombinant TNF-α was provided by TEBU.

TNF-α was quantified in cell supernatants by enzyme-linked immunosorbent assay (Genzyme), according to the manufacturer's protocol.

RNase protection assay. The RNase protection assay (PharMingen) was performed according to the supplier's instructions. Briefly, the human apoptosis template sets hAPO-2 and hAPO-3 were labeled with [α-^{32}P]uridine triphosphate. RNA (10 μg) and 8×10^5 cpm of labeled probes were used for hybridization. After RNase treatments, the protected probes were resolved on a 5% urea-polyacrylamide-bisacrylamide gel.

TUNEL immunostaining. Apoptosis was detected and quantified at the single-cell level by immunostaining by the terminal deoxynucleotidyltransferase-mediated dUTP nick end labeling (TUNEL) assay (Boehringer/Roche) according to the instructions of the assay kit manufacturer. DNA of fixed cells was labeled by adding fluorescein dUTP at strand breaks by terminal deoxynucleotidyl transferase, and detection and quantification were performed by fluorescence microscopy or flow cytometry.

Caspase activity assay. Caspase activity was assayed according to the protocol of the Biomol Quantizyme assay system. Cell extracts from primary erythroid CD36 cells and UT7-NS and UT7-pGRE cells were obtained by treating 10^6 cells in 50 μl of lysis buffer on ice and were incubated in assay buffer with either the caspase 3 substrate Ac-DEVD-pNA (*N*-acetyl-Asp-Glu-Val-Asp-*p*-nitroanilide) (200 μM) or the caspase 6 and 8 substrate Ac-IETD-pNA (*N*-acetyl-Ile-Glu-Thr-Asp-*p*-nitroanilide) (200 μM). The caspase-catalyzed release of *p*-nitroanilide was monitored at 405 nm in a microtiter plate reader. Cell extracts were treated with the caspase 3 inhibitor DEVD-CHO or the caspase 6 and 8 inhibitor IETD-CHO as a control.

Cell cycle analysis. Cells were pelleted by low-speed centrifugation, washed three times with ice-cold phosphate-buffered saline, fixed in 75% ice-cold ethanol, and stored at −20°C. After centrifugation, the cells were stained with 10 μg of propidium iodide/ml and counted in a Becton Dickinson FACS-Scan apparatus. Cell cycle profiles were examined by using the SOBR model to determine cellular distribution and the Cell Fit program (Becton Dickinson).

Ceramide assay. Ceramide was quantified by the diacylglycerol kinase assay as the amount of ^{32}P incorporated upon phosphorylation of ceramide to ceramide 1-phosphate by diacylglycerol kinase from *Escherichia coli* (Biomol) (13). The level of ceramide was determined by comparing the ^{32}P incorporation in cell lipid extracts to the concomitantly run standard curve plotted from known amounts of ceramide (Sigma) and normalized to [^{3}H]triglyceride introduced during lipid extraction.

Nuclear extract preparation and electrophoretic mobility shift assay. Nuclear extracts from CD36 and UT7 cells were prepared as previously described (55). The protein concentrations of the supernatants were determined by the micro-Bradford assay. Double-stranded oligonucleotides containing the NF-κB binding site (5′-AGCTTACAAGGGACTTTCCGCTA-3′) were labeled by filling in with the Klenow fragment of DNA polymerase I in the presence of [α-^{32}P]dCTP. Binding reactions took place at room temperature, with 5 μg of protein extract in the binding buffer (4% Ficoll, 20 mM HEPES [pH 7.5], 70 mM NaCl, 2 mM dithiothreitol, 100 μg of bovine serum albumin/ml, and 0.01% Nonidet P-40) and with 1 μg of poly(dI-dC) and 0.5 μg of salmon sperm DNA. After incubation at room temperature for 35 min, the reaction products were separated on a 5% acrylamide gel, which was then dried and autoradiographed. For competition experiments, a 20-fold excess of unlabeled NF-κB probe was added to the reaction mixture. In supershift experiments, 1 μl of antiserum to p50 or p65 was added 10 min before the probe. A control with antiserum and without protein was run. To quantify NF-κB binding activity, electrophoretic mobility shift assays were performed with a consensus Oct-1 probe (5′-AGCTTGTCGAATGCAAA TCACTAGAA-3′) under the same conditions. The nuclear DNA binding activity of NF-κB was quantified by phosphorimaging, and ratios were obtained by normalizing this activity to the level of the activity of the ubiquitous factor Oct-1.

RESULTS

Erythroid cell apoptosis induced by B19 infection or NS-1 expression. To explore the molecular mechanisms leading to erythroid cell death after natural infection by B19, we used purified normal human erythroid progenitors, i.e., $CD36^+$

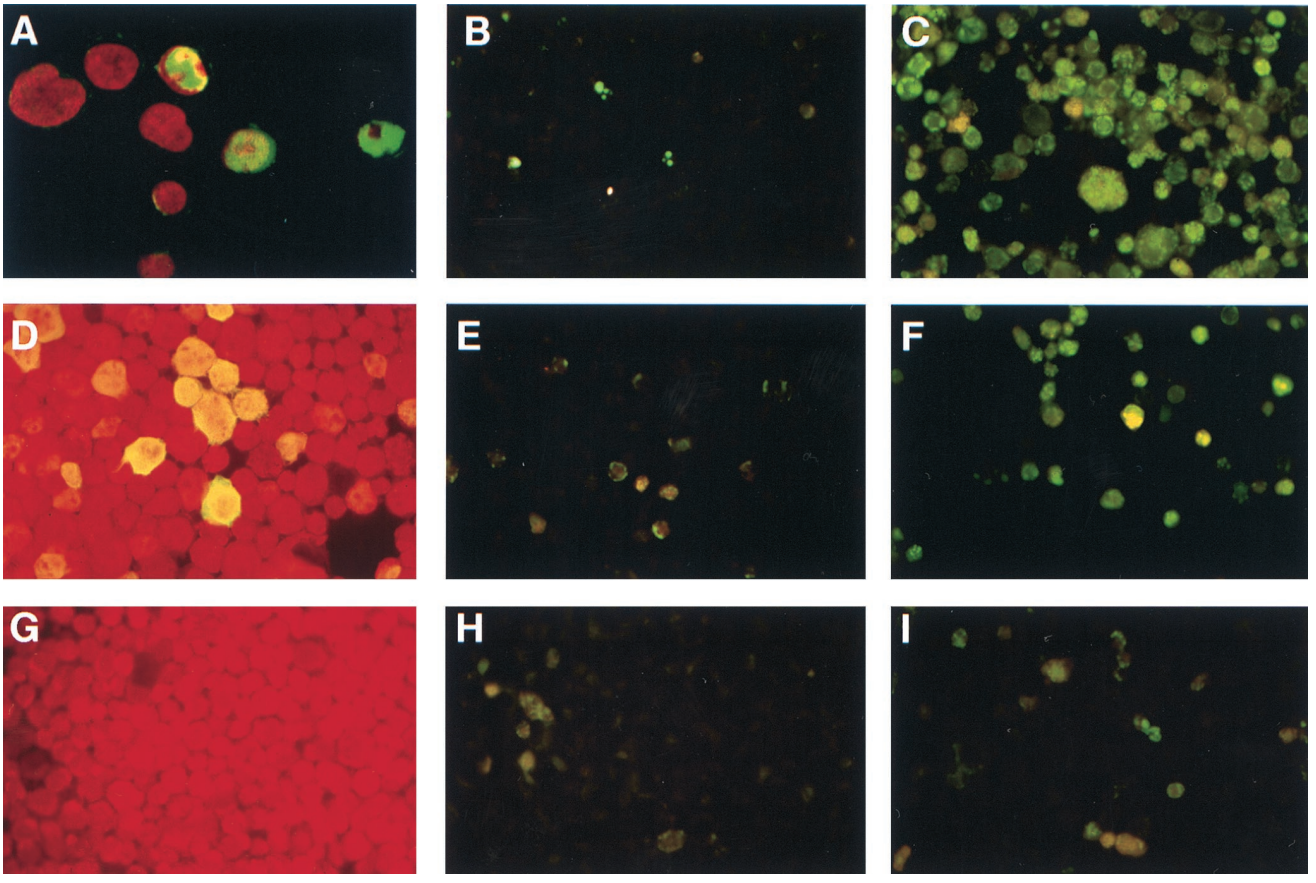

FIG. 1. (A) Expression of NS-1 protein in B19-infected CD36 cells. Magnification, ×400. The cells were fixed and incubated with a polyclonal rabbit anti-NS-1 antibody, and expression was revealed with monoclonal fluorescein isothiocyanate (FITC)-conjugated anti-rabbit Ig and then DAPI (4′,6-diamidino-2-phenylindole). Forty-eight hours after infection, NS-1 protein (green) was detected by confocal microscope analysis in the nucleus (red) and the cytoplasm in approximately 50% of the cells. (B) Apoptosis in uninfected CD36 cells. Magnification, ×250. Fragmented DNA of fixed cells was labeled by adding fluorescein dUTP, using the TUNEL assay. (C) Apoptosis in B19-infected CD36 cells 72 h after infection. (D) NS-1 protein expression in UT7-NS cells 48 h after its induction by DEX. The cells were fixed and incubated with a polyclonal rabbit anti-NS-1 antibody. NS-1 was revealed with monoclonal FITC-conjugated anti-rabbit Ig by immunofluorescence microscopy. (E) Apoptosis in uninduced UT7-NS cells. (F) Apoptosis in DEX-induced UT7-NS cells at 72 h. (G) UT7-pGRE cells incubated with a polyclonal rabbit anti-NS-1 antibody and a monoclonal FITC-conjugated anti-rabbit Ig antibody and then revealed by immunofluorescence microscopy. (H) Apoptosis in uninduced UT7-pGRE cells. (I) Apoptosis in DEX-induced UT7-pGRE cells.

cells. Twenty-four hours after CD36 cell infection with different B19 isolates, the capsid proteins and the nonstructural protein NS-1 were detectable by immunofluorescence in 50% of the cells. NS-1 was found in both the nucleus and the cytoplasm, as shown by confocal microscopic analysis (Fig. 1A). CD36 cells were also incubated with a noninfectious serum as a control. To determine whether apoptosis occurred in infected cells, we used TUNEL staining to identify cells with fragmented DNA. Apoptosis was not observed in uninfected CD36 cells (Fig. 1B). In contrast, apoptosis had occurred at 48 h after infection in 30% of B19-infected CD36 cells and at 72 h in 50% of infected cells (Fig. 1C and 2A), as confirmed by annexin V labeling (data not shown).

Several authors have suggested that the *NS* gene products encoded by B19 and other parvoviruses are involved in parvovirus-induced cytotoxicity (23, 25, 40, 48). Therefore, the UT7 erythroleukemia cell line, adapted for growth in Epo, was used to study the cytotoxicity of NS-1, in the framework of the erythroid-lineage cell. Constitutive expression of this protein in a stable cell line has not so far been possible, presumably because of its cytotoxicity. Therefore the *NS-1* gene was cloned under the control of a steroid-inducible promoter (24) and transfected into UT7 cells. We selected a stable cell clone (UT7-NS) expressing a high level of NS-1 after its induction by DEX, with 30% of the cells exhibiting specific nucleocytoplasmic staining by immunofluorescence (Fig. 1D). In this cell clone, the Epstein-Barr virus nuclear antigen 1 was detected in 90% of the cells by immunofluorescence (data not shown), and therefore, these cells possessed the NS-1 expression vector pGRE5-2/EBV-NS; however, DEX-induced NS-1 expression might also occur at a low level, undetectable by immunofluorescence. A UT7 erythroid cell line stably transfected with the empty vector pGRE5-2/EBV (UT7-pGRE) was also established as a control for the DEX effect. Apoptosis was not observed in UT7-pGRE cells treated with DEX (Fig. 1I). In contrast, when UT7-NS cells were induced to express NS-1 by DEX, apoptosis, measured 24, 48, and 72 h later by DNA fragmentation labeling, occurred at 48 h in 25% of UT7-NS cells and at 72 h in 40% of the cells (Fig. 1F and 2B).

These results suggest that cytotoxicity secondary to B19 infection of primary erythroid precursors involved an apoptotic process. It could have been induced by NS-1, since NS-1 expression induced apoptosis in the UT7 erythroid cell line.

Commitment to undergo apoptosis is associated with G_2 accumulation. Since deregulation of the cell cycle components may be involved in triggering apoptosis (20), we have explored

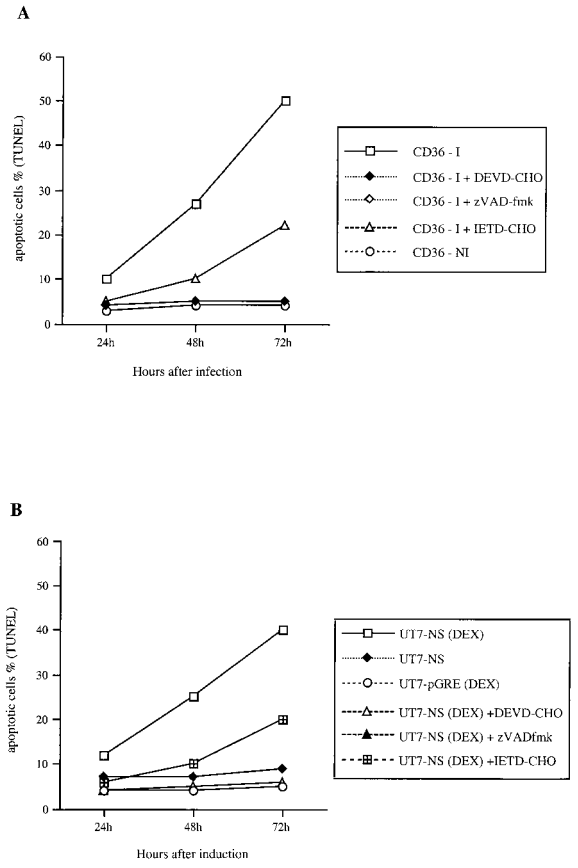

FIG. 2. (A) Apoptosis in B19-infected CD36 cells treated with caspase inhibitors. After B19 infection, infected CD36 cells (CD36-I) were cultured in the presence of DEVD-CHO, zVAD-fmk, or IETD-CHO. Uninfected CD36 cells (CD36-NI) were used as a control. At 24, 48, and 72 h, DNA fragmentation was determined by fluorescence microscopy, using the TUNEL assay. (B) NS-1-induced apoptosis in UT7-NS cells treated with caspase inhibitors. UT7-NS cells were induced to express NS-1 by DEX [UT7-NS (DEX)] and cultured in the presence of DEVD-CHO, zVAD-fmk, or IETD-CHO. Noninduced UT7-NS cells (UT7-NS) and UT7-pGRE cells induced by DEX [UT7-pGRE(DEX)] were used as controls. At 24, 48, and 72 h, DNA fragmentation was determined by fluorescence microscopy, using the TUNEL assay.

the impact of NS-1 expression on cell cycle progression. Analysis of the cycle of UT7-NS cells after NS-1 induction by DEX and that of UT7-pGRE cells treated with DEX showed an increase in the G_2/M fraction of UT7-NS cells 24 h after induction (47 versus 25% [Fig. 3A]), whereas control UT7-pGRE cells were distributed in equal proportions in G_1, S, and G_2/M. However, 48 and 72 h after induction, we found that the proportion of UT7-NS cells in G_2/M had decreased and was comparable to the proportion of UT7-pGRE cells (Fig. 3A). Therefore, in the UT7-NS cell line, NS-1-induced apoptosis was not associated with cell cycle arrest, but a transitory accumulation was observed in G_2/M.

Analysis of the cell cycles of infected and uninfected CD36 cells showed an increase in the number of cells in the G_2/M phase in infected versus uninfected cells 24 h after infection (40 versus 10% [Fig. 3B]), but the proportion of infected CD36 cells in G_2/M decreased at 48 h. A rise in the number of B19-infected cells with a sub-G_1 DNA content, which constituted the apoptotic cells, was found 48 h after infection.

Caspase activity involvement in B19- and NS-1-induced apoptosis. To ascertain whether the caspases participate in UT7-NS and CD36 cell apoptosis, CD36 cells infected with B19 and UT7-NS cells expressing NS-1 were treated with peptidic inhibitors of caspases. Apoptosis was almost completely inhibited by the broad-spectrum caspase inhibitor zVAD-fmk and the caspase 3 inhibitor DEVD-CHO and was 50% inhibited by the caspase 6 and 8 inhibitor IETD-CHO (Fig. 2).

Since B19- and NS-1-induced apoptosis was inhibited by caspase 3 and caspase 6 and 8 inhibitors, these caspase activities were evaluated in cellular extracts. Caspase 8 is at the apex of the caspase pathway and links death domain protein signaling to caspase activation (29), whereas caspase 3 is a critical downstream protease in the caspase cascade. Activated caspase 3 cleaves several cellular substrates and activates the endonucleases involved in DNA fragmentation (11, 37), and caspase 6 cleaves lamins and contributes to destruction of nuclear lamina (51). In vitro assays were performed with the caspase 6 and 8 substrate Ac-IETD-pNA, or a caspase 3 substrate, Ac-DEVD-pNA, in extracts of UT7-NS and UT7-pGRE cells induced by DEX and in extracts of uninfected or infected CD36 cells. The results at 48 h showed that substantial caspase 6 and 8 activities were induced by NS-1 expression in UT7-NS cells and were induced by B19 infection in CD36 cells (Fig. 4). Caspase 3 activity was also induced by NS-1 expression in UT7-NS cells and rose considerably in B19-infected CD36 cells (Fig. 4). No caspase 3 activity was induced by DEX in control UT7-pGRE cells, but a low level of caspase 3 activity was detected in uninfected CD36 cells. The caspase 6 and 8 inhibitor IETD-CHO abolished the cleavage of the substrate Ac-IETD-pNA, and the caspase 3 inhibitor DEVD-CHO abolished the cleavage of the substrate Ac-DEVD-pNA (data not shown).

These results suggest that B19- and NS-1-induced apoptosis involves caspase activity.

Absence of Fas-FasL interaction in B19- and NS-1-induced apoptosis. Since B19-induced apoptosis was apparently dependent on caspase 8 activity, which is upstream of the caspase pathway induced by TNFR1 and Fas (CD95), we explored the possibility that Fas ligand expression and subsequent Fas receptor ligation are involved in the mechanism of B19-induced apoptosis.

When Fas expression and FasL expression were evaluated at the RNA level by a ribonuclease protection assay, they were not detected in the UT7-NS cells, whether or not NS-1 expression was induced by DEX. In contrast, RNA transcripts from *fas* and *fasL* rose after B19 infection of CD36 cells (data not shown). However, in CD36 cells, Fas-FasL interaction is not involved in B19-induced apoptosis, since DNA fragmentation was not induced by the agonistic Fas antibody DX2 and was not inhibited by the antagonistic Fas antibody ZB4 (Fig. 5).

Erythroid cell sensitization by B19 and NS-1 to TNF-α-induced apoptosis. In contrast, apoptosis was enhanced by 18 h of treatment with 100 U of TNF-α/ml in both B19-infected CD36 cells and UT7-NS cells expressing NS-1 (Fig. 6), whereas primary CD36 and UT7-pGRE cells were resistant to TNF-α-induced apoptosis. As this sensitivity to TNF-α might have been due to an increase in TNFR1 expression, the level of this expression was evaluated by indirect immunofluorescence and flow cytometry. However, the TNFR1 level rose only slightly at the cell surface in UT7-NS and infected CD36 cells (data not shown), suggesting that the effects of B19 and NS-1 were not due to increased TNFR1 expression. Moreover, TNF-α was not found in supernatants from infected CD36 cells or UT7-NS cells with DEX-induced NS-1 expression, and RNA transcripts from *TNF* were not detected by reverse transcription-PCR. Alternatively, NS-1 might modulate TNFR1 signaling by direct interaction with some component of the transduction pathway downstream of TNFR1.

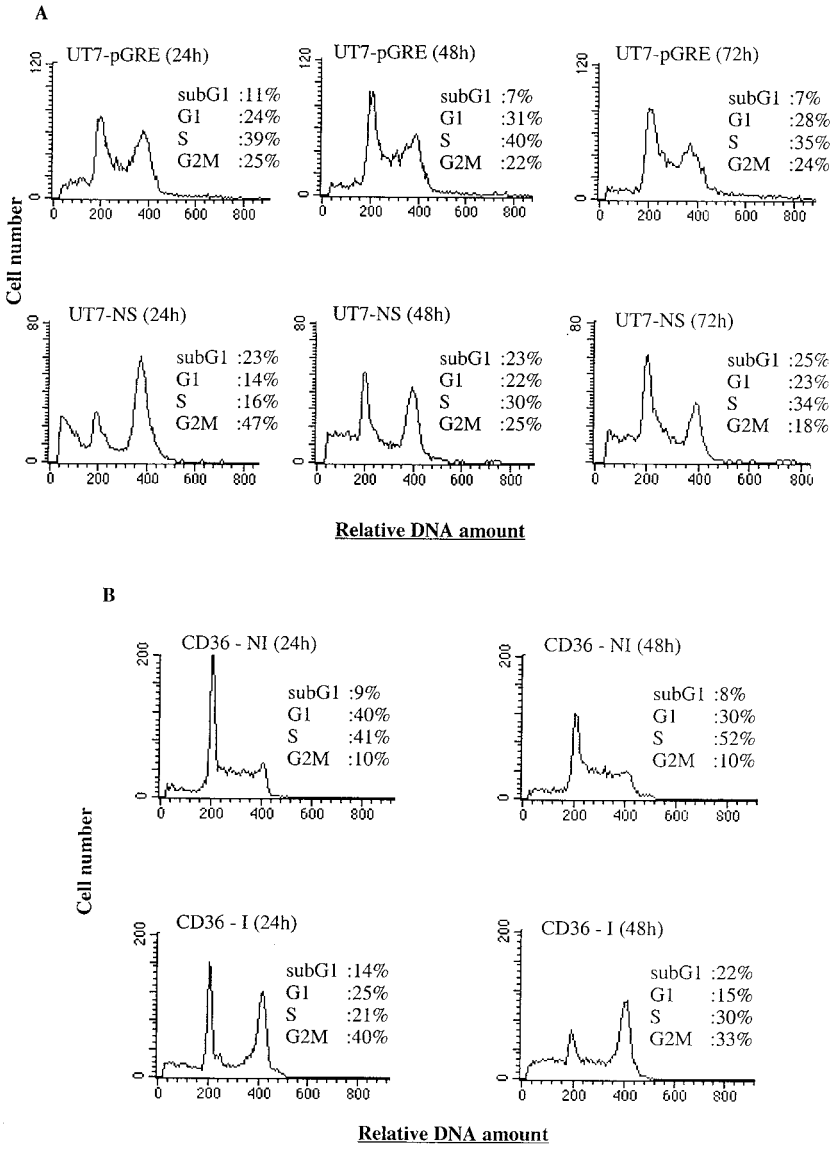

FIG. 3. UT7-NS- and B19-infected CD36 cell cycles. FACS-Scan demonstrating that cell cycle progression is modified by the expression of NS-1 protein in the erythroleukemia cell line UT7-NS (A) or by B19 infection in primary CD36 cells (B). At different times after the induction of NS-1 expression (A) or B19 infection (B), the cells were harvested and cellular DNA content was assayed. The data in panels A and B are from the same experiment, representative of two independent experiments with similar results.

Ceramide production in B19- and NS-1-induced apoptosis. Among the signals leading to TNF-induced cell death, the activation of acidic sphingomyelinase and the subsequent ceramide production have often been reported (1, 43, 45). We investigated the possibility that B19 infection and NS-1 expression generate ceramide production and found that in lipid extracts from B19-infected CD36 cells, the ceramide level had risen by 280% 24 h after infection and by 440% at 48 h. In lipid extracts from UT7-NS cells with DEX-induced NS-1 expression, 18 h after DEX treatment, the ceramide level had risen by 180%, whereas in DEX-treated UT7-pGRE cell extracts it was unchanged (Fig. 7A). B19 infection and NS-1 protein expression therefore enhanced ceramide production.

To determine whether ceramide itself triggers DNA fragmentation, UT7-NS, UT7-pGRE, and CD36 cells were treated with 10 μM C2-ceramide (a short chain, cell-permeable analog of ceramide), and TUNEL assays were performed 24, 48, and 72 h later. C2-ceramide treatment had no effect on UT7-pGRE cells but dramatically increased DNA fragmentation in UT7-NS cells expressing NS-1 (Fig. 7B). Moreover, C2-ceramide induced apoptosis in primary CD36 cells in the absence of infection. Because C2-ceramide is an amphiphilic lipid analog that may have nonspecific activities, it was important to check its specificity of action. Accordingly, we tested the effect of C2-dihydroceramide (a structural analog of C2-ceramide) at the same concentration and found that it was inactive (data not shown), thus demonstrating the specificity of action of C2-ceramide. Therefore, ceramide induced apoptosis in primary erythroid cells but only enhanced NS-1 protein-induced DNA fragmentation in UT7 erythroid cells. These results suggest that when ceramide is generated by NS-1 expression, it might be a factor contributing to erythroid cell death.

NF-κB activation in B19- and NS-1-induced apoptosis. We found that UT7 erythroid cells and primary CD36 cells were

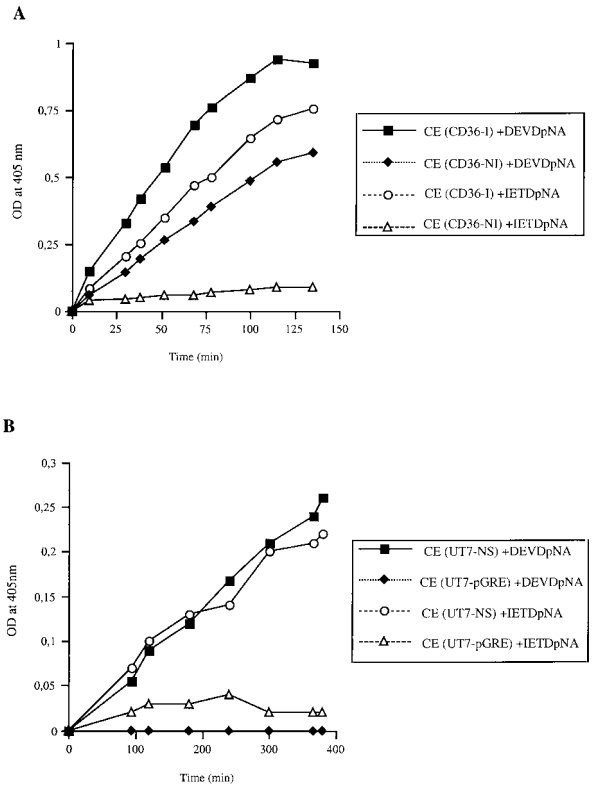

FIG. 4. Determination of caspase 3, 6, and 8 activities. (A) Cell extracts were obtained 48 h after B19 infection of CD36 cells [CE(CD36-I)] and from uninfected CD36 cells [CE(CD36-NI)]. Extracts were assayed for caspase 3 activity toward the peptide substrate Ac-DEVD-pNA and for caspase 6 and caspase 8 activities toward the peptide substrate Ac-IETD-pNA. (B) Cell extracts from UT7-NS cells induced to express NS-1 by DEX or from UT7-pGRE cells treated with DEX for 48 h were assayed for caspase 3 activity toward the peptide substrate Ac-DEVD-pNA. The extracts were also assayed for caspase 6 and 8 activities toward the peptide substrate Ac-IETD-pNA. The experiments were performed in duplicate, and the data are from the same experiment, representative of two independent experiments with similar results. OD, optical density.

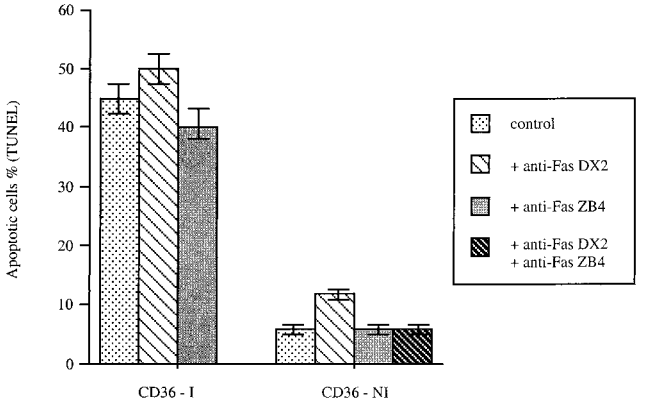

FIG. 5. Effect of the anti-Fas agonistic antibody DX2 or antagonistic antibody ZB4 on infected or uninfected CD36 cells. After B19 infection, CD36 cells (CD36-I) were cultured in the presence of DX2 antibody (100 ng/ml) or ZB4 antibody (500 ng/ml) or without antibody as a control. Noninfected CD36 cells (CD36-NI) were also cultured in the presence of DX2 (100 ng/ml), ZB4 (500 ng/ml), or DX2 and ZB4 or without antibody as a control. Forty hours after infection, the cells were harvested and apoptosis was measured by TUNEL assay. The data are means ± standard errors of three separate experiments.

resistant to TNF-α cytotoxicity and that B19 infection and NS-1 expression induced TNF-α sensitivity. Several authors have demonstrated that cellular resistance to TNF-α requires TRAF-2, which acts mainly by mediating the activation of the transcription factor NF-κB (26). Since we had explored the possible modulation of TNFR1 signaling by NS-1, we also investigated the possible role of NS-1 in the activation of NF-κB by performing electrophoretic mobility shift assays on nuclear extracts of UT7-pGRE and UT7-NS cells induced by DEX and infected and uninfected CD36 cells, using a ^{32}P-labeled DNA probe encompassing a consensus site for NF-κB. NF-κB complexes were almost undetectable in nuclear extracts of UT7-pGRE and UT7-NS cells expressing DEX-induced NS-1 but were detected 24 h after TNF-α treatment, in both UT7-pGRE and UT7-NS cells expressing NS-1 (Fig. 8A). Similar results were obtained at 48 h after induction by DEX (data not shown). In contrast, in CD36 cell extracts, the nuclear DNA binding activity of NF-κB had increased 16-fold 24 h after infection compared with the activity in uninfected control cells (Fig. 8A). The specificity of NF-κB transcription factor binding was confirmed by a competition assay performed with a 20-fold excess of unlabeled probe, as well as by supershift experiments with antibodies directed toward the p50 and p65 subunits of NF-κB (Fig. 8B). These results showed that in the UT7-NS cells NF-κB activity is not modified by NS-1 expression, and they therefore suggest that sensitivity to TNF-α cytotoxicity did not involve the inhibition of TNF-α-induced NF-κB activity. In contrast, B19 infection enhanced NF-κB activity in primary CD36 cells.

DISCUSSION

We studied the mechanism of erythroid toxicity induced by B19, which targets BFU-E and CFU-E cells. Previous reports suggested that the *NS* gene products encoded by various parvoviruses possessing homologous domains (H-1 virus, minute virus of mice [MVM], and B19) have cytotoxic activities (23, 25, 31, 40, 48). We therefore evaluated the impact of NS-1 in the UT7 erythroleukemia cell line stably expressing the NS-1 protein. Our findings indicate that B19 infection of CD36 cells, which at the BFU-E–CFU-E stage are primary erythroid precursors, clearly induced apoptosis. Since NS-1 expression also induced apoptosis in UT7-NS erythroid cells, it seemed likely that NS-1 is involved in B19-induced apoptosis as well.

This apoptosis does not seem to be associated with cell cycle arrest but with an accumulation of B19-infected C36 cells in the G_2/M phase of the cell cycle. Similar results were observed with the NS-1 protein in UT7-NS cells. The NS-1 protein of MVM also induced G_2/M accumulation, but the mechanism(s) by which this protein alters the duration of the G_2 phase is still not clear (39). As a transcription regulator, NS-1 might exert its cytostatic activity by regulating the expression of factors involved in cell cycle control (20).

Since we found here that NS-1-induced apoptosis in erythroid progenitor cells was inhibited by the caspase inhibitors zVAD-fmk and DEVD-CHO, this apoptosis did involve caspase activation. Caspases are synthesized as precursors that undergo proteolytic maturation, and a cascade model has been suggested for effector caspase activation resulting in cellular disassembly (54). Different initiator caspases mediate distinct sets of signals. Caspase 6, 8, and 3 activities, which increased here in cells expressing NS-1, are associated with apoptosis involving death receptors (2). The best-characterized death receptors are CD95 (Fas) and TNFR1. Fas expression at the surfaces of infected erythroid cells might occur, as well as cross-linking with FasL, which is constitutively expressed

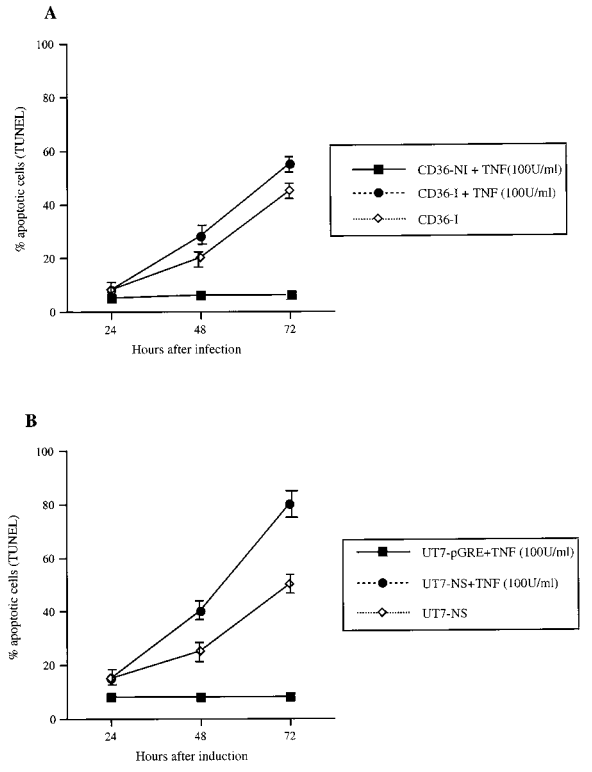

FIG. 6. Effect of TNF-α treatment on B19- and NS-1-induced apoptosis. (A) Effect of TNF-α treatment on B19-induced apoptosis. Infected CD36 cells (CD36-I) or uninfected cells (CD36-NI) were treated with 100 U of TNF-α/ml for 18 h. Apoptosis was evaluated by TUNEL assay 24, 48, and 72 h after infection. (B) Effect of TNF-α treatment on NS-1-induced UT7-NS cell apoptosis. UT7-NS and UT7-pGRE cells were treated with DEX and then with 100 U of TNF-α for 18 h. Apoptosis was determined by TUNEL assay 24, 48, and 72 h after infection. The data are means ± standard errors of three separate experiments.

among erythroid progenitors, thus inducing apoptosis. Such a mechanism has been proposed for the erythroid cell apoptosis induced by gamma interferon (8, 28). Although Fas expression and FasL expression were enhanced here in B19-infected CD36 cells, this pathway does not seem to play a role in B19-induced apoptosis ex vivo, as shown by the absence of effect of agonist and antagonist Fas antibodies on DNA fragmentation. Previous reports suggested that, as for many other death pathways, the cellular background plays an essential role in the interpretation and modulation of the Fas-generating signal (9, 36). Thus, cell sensitivity or resistance involves factors other than the level of expression of Fas. In contrast, Fas-FasL expression was not detected in the erythroid cell line expressing NS-1, either by us or by others (31), and therefore NS-1 induced apoptosis in the absence of Fas-FasL.

As the hypothesis of Fas-mediated death was not considered likely, the involvement of TNFR1 was explored. The involvement of TNFR1 signaling was suggested by the enhancement of B19- and NS1-induced apoptosis after TNF-α treatment. Thus, we found that when CD36 cells were cultured with SCF, IL-3, IL-6, and Epo, they were resistant to TNF-α-induced cytotoxicity but that infection by B19 sensitized CD36 cells to TNF-α-induced apoptosis. TNF-α has been demonstrated to signal both the inhibition and stimulation of hematopoietic progenitor cells, depending on the growth factors it interacts with and on the concentration of TNF-α in the culture medium (28, 44). Since in the present experiments cell sensitivity to TNF-α was not due to the upregulation of TNFR1 or TNF-α expression, NS-1 might modulate TNFR1 signaling by direct interaction with certain components of the transduction pathway downstream of TNFR1. Among the signals leading to TNF-induced cell death, the activation of acidic sphingomyelinase and the subsequent ceramide production have very often been reported (1, 43, 45), and we indeed found that B19 infection and NS-1 expression generated ceramide production. In addition, we demonstrated that exogenously added permeant C2-ceramide induces apoptosis in primary CD36 cells and increases apoptosis in UT7 erythroid cells expressing the NS-1 protein. These results strengthen the hypothesis that there is a connection between the TNFR1 apoptotic pathway

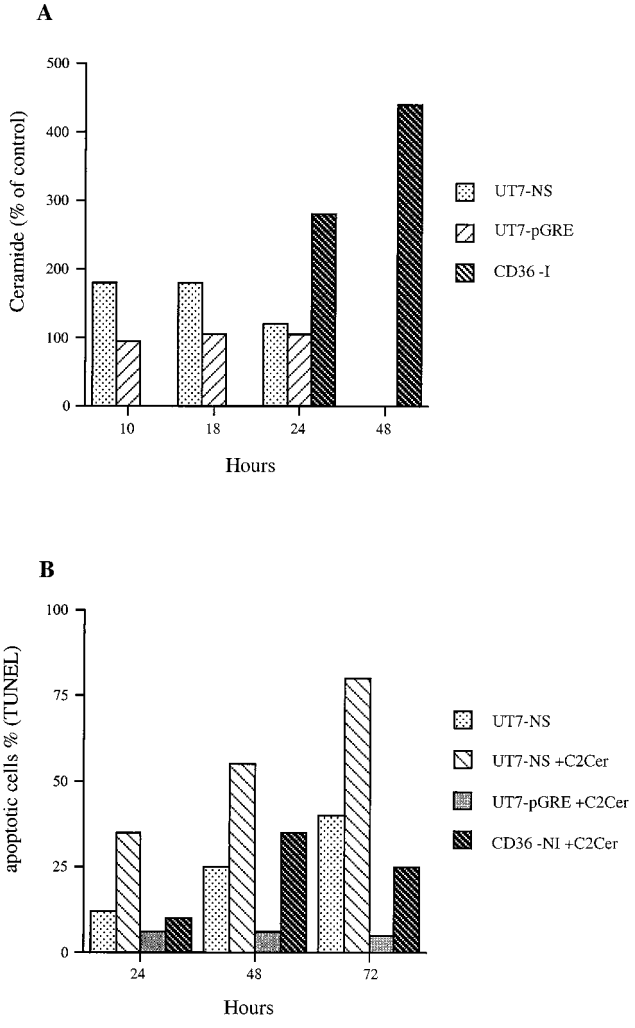

FIG. 7. (A) Time course of ceramide production after induction of NS-1 protein expression and B19 infection. NS-1 expression was induced in UT7-NS cells by DEX, UT7-pGRE cells were treated with DEX, and noninduced UT7-NS and UT7-pGRE cells were used as controls; 10, 18, and 24 h thereafter, ceramide production was quantified by diacylglycerol kinase assay in cell lipid extracts. Ceramide production was also quantified 24 and 48 h after infection in B19-infected CD36 cells, with uninfected CD36 cells as a control. (B) Apoptosis induced by C2-ceramide treatment of UT7-NS cells expressing NS-1 and CD36 cells. NS-1 expression was induced in UT7-NS cells by DEX, and UT7-pGRE cells were treated with DEX, and the cells were then treated with 10 μM C2-ceramide (C2cer). Uninfected CD36 cells were also treated with 10 μM C2-ceramide. Apoptosis was quantified by TUNEL assay at 24, 48, and 72 h thereafter. The data in panels A and B are from the same experiment, representative of two independent experiments with similar results.

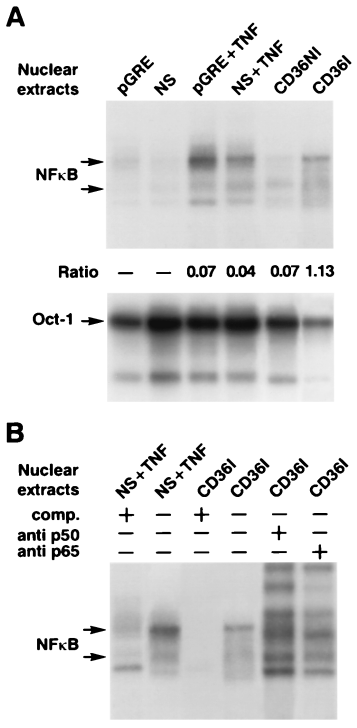

FIG. 8. Electrophoretic mobility gel shift analysis. (A) Equivalent amounts (5 μg) of nuclear extracts were prepared from UT7-pGRE cells treated with DEX, UT7-NS cells with DEX-induced NS-1 protein expression, and infected or uninfected CD36 cells. Binding of NF-κB or Oct-1 ubiquitous transcription factor was determined with a ^{32}P-labeled DNA probe encompassing a consensus site for NF-κB or Oct-1. NF-κB activity was quantified by phosphorimaging, and ratios were obtained by normalizing the activities to the level of activity of Oct-1. Nuclear extracts from UT7-pGRE (pGRE) and UT7-NS (NS) cells, UT7-pGRE and UT7-NS cells treated with 100 U of TNF-α/ml (+TNF), uninfected CD36 cells (CD36NI), and B19-infected CD36 cells (CD36I) were measured. (B) Competition binding of nuclear extracts with a 20-fold excess of probe is shown for UT7-NS cells treated with TNF (NS + TNF) and B19-infected CD36 cells (CD36I). Supershift analysis is shown for B19-infected CD36 cell extracts incubated with an antibody directed toward the p50 and p65 subunits of NF-κB, respectively (two right lanes). +, present; −, absent; comp., competitor.

and B19. Apoptosis was also involved in the death of monocytic U937 cells infected with parvovirus H-1 (42). The apoptotic pathway triggered by this parvovirus appears to have at least some steps in common with the one activated by TNF-α, as is especially clear from the resistance to TNF of cell variants selected for their ability to survive virus infection. Treatment of U937 cells with TNF-α, or their infection by H-1 parvovirus, was observed to be accompanied by fast and drastic downregulation of c-Myc expression, prior to the appearance of apoptotic signs (42).

The detection of increased NF-κB binding activity in B19-induced apoptosis of erythroid cells was more tricky to interpret. Signaling by TNFR1 results in phosphorylation and subsequent degradation of the inhibitory proteins of NF-κB called IκBs, allowing NF-κB to translocate into the nucleus and activate target genes (49). Direct interference by NS-1 with the phosphorylation of IκBs cannot be excluded, since NS-1 is a serine-threonine-phosphorylated protein (19), as described for other viral proteins (50). NS-1 phosphorylation might explain the discrepancy between NF-κB activation in B19-infected CD36 cells and in NS-1-expressing UT7-NS cells. Alternatively, other proteins encoded by B19 might induce NF-κB activity (27), and we are now investigating this possibility.

In the absence of TNF-α in the supernatants of CD36-infected and NS-1-expressing UT7 cells, the involvement of the TNFR1 pathway during NS-1-induced apoptosis might result from the interaction of NS-1 with the death domain of TNFR1 and/or TRADD, leading to the activation of the two major TNF-α signaling pathways that induce apoptosis and NF-κB activation, respectively. Direct interactions of viral proteins with the death domain of TNFR1 or FADD have already been described and might enhance or inhibit TNF-induced apoptosis (53, 57). The death receptor 3 (DR3; also called WSL-1) also triggers responses that resemble those of TNFR1, namely, NF-κB activation and caspase-dependent apoptosis. Nevertheless, DR3 transcripts have so far mainly been described in the spleen, thymus, and peripheral blood (21).

Gene products of the Bcl-2 family are key regulators of programmed cell death, and some proteins promote it, whereas others, like Bcl-X_L and Mcl-1, exert a protective effect (46). Bcl-X-deficient mice died in utero as a result of the massive death of erythroid cells (35). As the nonstructural protein of MVM induces promoter inhibition of cellular genes (23), the possibility that NS-1 downregulates Bcl-X_L and Mcl-1 transcription cannot be excluded. Nevertheless, the dysregulation of Bcl-X_L and Mcl-1 expression at the RNA and protein levels was not observed here, either in erythroid cells infected by B19 or in erythroid cells expressing the *NS-1* gene (data not shown).

In conclusion, our data suggest that the induction of erythroid cell apoptosis by B19 at least involves the TNFR1 signaling pathway. Further research is necessary to clarify the ways in which NS-1 might interact with the proteins of such signaling pathways, either directly or by their phosphorylation.

ACKNOWLEDGMENTS

We thank C. Gazin (Inserm U462, Paris, France), M. Neves, and A. Saib (CNRS UPR 9051, Paris, France) for helpful advice and discussion. We thank N. Rice (Frederick Cancer Research and Development Center) for the generous gift of antibodies against the p50 and p65 subunits of NF-κB. Last, we are indebted to the Laboratoire Photographique d'Hématologie for photographic work, M. Schmid and C. Doliger for scanning densitometry analysis, and M. C. Daudon for editorial assistance.

REFERENCES

1. **Adam-Klages, S., R. Schwandner, D. Adam, D. Kreder, K. Bernardo, and M. Krönke.** 1998. Distinct adapter proteins mediate acid versus neutral sphingomyelinase activation through the p55 receptor for tumor necrosis factor. J. Leukoc. Biol. **63:**678–682.
2. **Ashkenazi, A., and V. M. Dixit.** 1998. Death receptors: signaling and modulation. Science **281:**1305–1308.
3. **Baeuerle, P. A., and D. Baltimore.** 1996. NF-κB: ten years after. Cell **87:**13–20.
4. **Beg, A. A., and D. Baltimore.** 1996. An essential role for NF-κB in preventing TNF-alpha induced cell death. Science **274:**782–784.
5. **Chinnaiyan, A. M., K. O'Rourke, M. Tewari, and V. M. Dixit.** 1995. FADD, a novel death domain-containing protein, interacts with the death domain of Fas and initiates apoptosis. Cell **81:**505–514.
6. **Cotmore, S. F., V. C. McKie, L. J. Anderson, C. R. Astell, and P. Tattersall.** 1986. Identification of the major structural and nonstructural proteins encoded by human parvovirus B19 and mapping of their genes by procaryotic expression of isolated genomic fragments. J. Virol. **60:**548–557.
7. **Cotmore, S. F., and P. Tattersall.** 1984. Characterization and molecular cloning of a human parvovirus genome. Science **226:**1161–1165.
8. **Dai, C. H., J. O. Price, T. Brunner, and S. B. Krantz.** 1998. Fas ligand is present in human erythroid colony-forming cells and interacts with Fas induced by interferon γ to produce erythroid cell apoptosis. Blood **91:**1235–1242.
9. **De Maria, R., U. Testa, L. Luchetti, A. Zeuner, G. Stassi, E. Pelosi, R. Riccioni, N. Felli, P. Samoggia, and C. Peschle.** 1999. Apoptotic role of Fas/Fasligand system in the regulation of erythropoiesis. Blood **93:**796–803.
10. **Doerig, C., B. Hirt, J. P. Antonietti, and P. Beard.** 1990. Nonstructural protein of parvoviruses B19 and minute virus of mice controls transcription. J. Virol. **64:**387–396.
11. **Enari, M., H. Sakahira, H. Yokoyama, K. Okawa, A. Iwamatsu, and S.**

Nagata. 1998. A caspase-activated DNase that degrades DNA during apoptosis, and its inhibitor ICAD. Nature **391:**43–50.
12. **Enari, M., R. V. Talanian, W. W. Wong, and S. Nagata.** 1996. Sequential activation of ICE-like and CPP32-like proteases during Fas-mediated apoptosis. Nature **380:**723–726.
13. **Genestier, L., A. F. Prigent, R. Paillot, L. Quemeneur, I. Durand, J. Banchereau, J. P. Revillard, and N. Bonnefoy-Bérard.** 1998. Caspase-dependent ceramide production in Fas- and HLA class I-mediated peripheral T cell apoptosis. J. Biol. Chem. **273:**5060–5066.
14. **Green, D. R.** 1998. Apoptotic pathways: the roads to ruin. Cell **94:**695–698.
15. **Hannun, Y. A.** 1996. Functions of ceramide in coordinating cellular responses to stress. Science **274:**1855–1859.
16. **Hsu, H., H. B. Shu, M. G. Pan, and D. V. Goeddel.** 1996. TRADD-TRAF2 and TRADD-FADD interactions define two distinct TNF receptor 1 signal transduction pathways. Cell **84:**299–308.
17. **Hsu, H., J. Xiong, and D. V. Goeddel.** 1995. The TNF receptor 1-associated protein TRADD signals cell death and NF-κB activation. Cell **81:**495–504.
18. **Jarvis, W. D., R. N. Kolesnick, F. A. Fornari, R. S. Traylor, D. A. Gewirtz, and S. Grant.** 1994. Induction of apoptotic DNA damage and cell death by activation of the sphingomyelin pathway. Proc. Natl. Acad. Sci. USA **91:**73–77.
19. **Kawase, M., K. Itoh, M. Momoeda, N. S. Young, and S. Kajigaya.** 1995. Phosphorylation of B19 parvovirus nonstructural protein, p. 104. *In* Proceedings of the VIth Parvovirus Workshop, Montpellier, France.
20. **King, K. L., and J. A. Cidlowski.** 1995. Cell cycle and apoptosis: common pathways to life and death. J. Cell. Biochem. **58:**175–180.
21. **Kitson, J., T. Raven, Y.-P. Jiang, D. V. Goeddel, K. M. Giles, K.-T. Pun, C. J. Grinham, R. Brown, and S. N. Farrow.** 1996. A death-domain-containing receptor that mediates apoptosis. Nature **384:**372–375.
22. **Lecoq-Lafon, C., J. M. Freyssinier, F. Picard, R. Ducrocq, P. Mayeux, C. Lacombe, and S. Fichelson.** Purification, amplification and characterization of a pure population of human erythroid progenitors. Br. J. Haematol., in press.
23. **Legendre, D., and J. Rommelaere.** 1992. Terminal regions of the NS1 protein of the parvovirus minute virus of mice are involved in cytotoxicity and promoter transinhibition. J. Virol. **66:**5705–5713.
24. **Leruez-Ville, M., I. Vassias, C. Pallier, A. Cecille, U. Hazan, and F. Morinet.** 1997. Establishment of a cell line expressing human parvovirus B19 nonstructural protein from an inducible promoter. J. Gen. Virol. **78:**215–219.
25. **Li, X., and S. L. Rhode.** 1990. Mutation of lysine 405 to serine in the parvovirus H-1 NS1 abolishes its functions for viral DNA replication, late promoter transactivation, and cytotoxicity. J. Virol. **64:**4654–4660.
26. **Liu, Z. G., H. Hsu, D. V. Goeddel, and M. Karin.** 1996. Dissection of TNF receptor 1 effector functions: JNK activation is not linked to apoptosis while NF-κB activation prevents cell death. Cell **87:**565–576.
27. **Luo, W., and C. R. Astell.** 1993. A novel protein encoded by small RNAs of parvovirus B19. Virology **195:**448–455.
28. **Maciejewski, J., C. Selleri, S. Anderson, and N. S. Young.** 1995. Fas antigen expression on CD34+ human marrow cells is induced by interferon gamma and tumor necrosis factor alpha and potentiates cytokine-mediated hematopoietic suppression in vitro. Blood **85:**3183–3190.
29. **Medema, J. P., C. Scaffidi, F. C. Kischkel, A. Shevchenko, M. Mann, P. H. Krammer, and M. E. Peter.** 1997. FLICE is activated by association with the CD95 death-inducing signaling complex (DISC). EMBO J. **16:**2794–2802.
30. **Moffatt, S., N. Tanaka, K. Tada, M. Nose, M. Nakamura, O. Muraoka, T. Hirano, and K. Sugamura.** 1996. A cytotoxic nonstructural protein NS1 of human parvovirus B19 induces activation of interleukin-6 gene expression. J. Virol. **70:**8485–8491.
31. **Moffatt, S., N. Yaegashi, K. Tada, N. Tanaka, and K. Sugamura.** 1998. Human parvovirus B19 nonstructural protein NS1 induces apoptosis in erythroid lineage cells. J. Virol. **72:**3018–3028.
32. **Momoeda, M., S. Wong, M. Kawase, N. S. Young, and S. Kajigaya.** 1994. A putative nucleoside triphosphate-binding domain in the nonstructural protein of B19 parvovirus is required for cytotoxicity. J. Virol. **68:**8443–8446.
33. **Morey, A. L., D. J. Ferguson, and K. A. Fleming.** 1993. Ultrastructural features of fetal erythroid precursors infected with parvovirus B19 in vitro: evidence of cell death by apoptosis. J. Pathol. **169:**213–220.
34. **Mortimer, P. P., R. K. Humphries, J. G. Moore, R. H. Purcell, and N. S. Young.** 1983. A human parvovirus-like virus inhibits haematopoietic colony formation in vitro. Nature **302:**426–429.
35. **Motoyama, N., F. Wang, K. A. Roth, H. Sawa, K. Nakayama, I. Negishi, S. Senju, Q. Zhang, S. Fujii, and D. Y. Loh.** 1995. Massive cell death of immature hematopoietic cells and neurons in Bcl-X-deficient mice. Science **267:**1506–1509.
36. **Nagata, S., and P. Golstein.** 1995. The Fas death factor. Science **267:**1449–1456.
37. **Nicholson, D. W., A. Ali, N. A. Thornberry, J. P. Vaillancourt, C. K. Ding, M. Gallant, Y. Gareau, P. R. Griffin, M. Labelle, Y. A. Lazebnik, N. A. Munday, S. M. Raju, M. E. Smulson, T. T. Yamin, V. L. Yu, and D. K. Miller.** 1995. Identification and inhibition of the ICE/CED-3 protease necessary for mammalian apoptosis. Nature **376:**37–43.
38. **Obeid, L. M., C. M. Linardic, L. A. Karolak, and Y. Hannun.** 1993. Programmed cell death induced by ceramide. Science **259:**1769–1771.
39. **Op De Beeck, A., F. Anouja, S. Mousset, J. Rommelaere, and P. Caillet-Fauquet.** 1995. The nonstructural proteins of the autonomous parvovirus minute virus of mice interfere with the cell cycle, inducing accumulation in G2. Cell Growth Differ **6:**781–787.
40. **Ozawa, K., J. Ayub, S. Kajigaya, T. Shimada, and N. Young.** 1988. The gene encoding the nonstructural protein of B19 human parvovirus may be lethal in transfected cells. J. Virol. **62:**2884–2889.
41. **Pallier, C., A. Greco, J. J. Le, A. Saib, I. Vassias, and F. Morinet.** 1997. The 3′ untranslated region of the B19 parvovirus capsid protein mRNAs inhibits its own mRNA translation in nonpermissive cells. J. Virol. **71:**9482–9489.
42. **Rayet, B., L. Lopez-Guerrero, J. Rommelaere, and C. Dinsart.** 1998. Induction of programmed cell death by parvovirus H-1 in U937 cells: connection with the tumor necrosis factor alpha signalling pathway. J. Virol. **72:**8893–8903.
43. **Rivas, C. I., J. C. Golde, J. C. Vera, and R. N. Kolesnick.** 1994. Involvement of the sphingomyelin pathway in autocrine tumor necrosis factor signaling for human immunodeficiency virus production in chronically infected HL-60 cells. Blood **83:**2191–2197.
44. **Rusten, L. S., and S. E. W. Jacobsen.** 1995. Tumor necrosis factor (TNF)-alpha directly inhibits human erythropoiesis in vitro: role of p55 and p75 TNF receptors. Blood **85:**989–996.
45. **Schwander, R., K. Wiegmann, K. Bernardo, D. Kreder, and M. Krönke.** 1998. TNF receptor death domain-associated proteins TRADD and FADD signal activation of acid sphingomyelinase. J. Biol. Chem. **273:**5916–5922.
46. **Silva, M., D. Grillot, A. Benito, C. Richard, G. Nunez, and J. L. Fernandez-Luna.** 1996. Erythropoietin can promote erythroid progenitor survival by repressing apoptosis through Bcl-XL and Bcl-2. Blood **88:**1576–1582.
47. **Sol, N., F. Morinet, M. Alizon, and U. Hazan.** 1993. Trans-activation of the long terminal repeat of human immunodeficiency virus type 1 by the parvovirus B19 NS1 gene product. J. Gen. Virol. **74:**2011–2014.
48. **Srivastava, A., E. Bruno, R. Briddell, R. Cooper, C. Srivastava, K. van Besien, and R. Hoffman.** 1990. Parvovirus B19-induced perturbation of human megakaryocytopoiesis *in vitro*. Blood **76:**1997–2004.
49. **Stancovski, I., and D. Baltimore.** 1997. NF-κB activation: the IκB kinase revealed. Cell **91:**299–302.
50. **Sylla, B. S., S. C. Hung, D. M. Davidson, E. Hatzivassiliou, N. L. Malinin, D. Wallach, T. D. Gilmore, E. Kieff, and G. Mosialos.** 1998. Epstein-Barr virus-transforming protein latent membrane protein 1 activates transcription factor NF-kappa B through a pathway that includes the NF-kappa B-inducing kinase and the IkappaB kinases IKKalpha and IKKbeta. Proc. Natl. Acad. Sci. USA **95:**10106–10111.
51. **Takahashi, A., E. S. Alnemri, Y. A. Lazebnik, T. Fernandes-Alnemri, G. Litwack, R. D. Moir, R. D. Goldman, G. G. Poirier, S. H. Kaufmann, and W. C. Earnshaw.** 1996. Cleavage of lamin A by Mch2a but not CPP32: multiple interleukin 1 beta-converting enzyme-related proteases with distinct substrate recognition properties are active in apoptosis. Proc. Natl. Acad. Sci. USA **93:**8395–8400.
52. **Tewari, M., and V. M. Dixit.** 1995. Fas- and tumor necrosis factor-induced apoptosis is inhibited by the poxvirus crmA gene product. J. Biol. Chem. **270:**3255–3260.
53. **Thome, M., P. Schneider, K. Hofmann, H. Fickenscher, E. Meinl, F. Neipel, C. Mattmann, K. Burns, J.-L. Bodmer, M. Schröter, C. Scaffidi, P. H. Krammer, M. E. Peter, and J. Tschopp.** 1997. Viral FLICE-inhibitory proteins (FLIPs) prevent apoptosis induced by death receptors. Nature **386:**517–521.
54. **Thornberry, N. A., and Y. Lazebnik.** 1998. Caspases: enemies within. Science **281:**1312–1316.
55. **Vassias, I., U. Hazan, Y. Michel, C. Sawa, H. Handa, L. Gouya, and F. Morinet.** 1998. Regulation of human B19 parvovirus promoter expression by hGABP (E4TF1) transcription factor. J. Biol. Chem. **273:**8287–8293.
56. **Young, N. S.** B19 parvovirus, p. 75–177. *In* N. S. Young (ed.), Viruses and bone marrow. Marcel Dekker, New York, N.Y.
57. **Zhu, N., A. Khoshnan, R. Schneider, M. Matsumoto, G. Dennert, C. Ware, and M. M. C. Lai.** 1998. Hepatitis C virus core protein binds to the cytoplasmic domain of tumor necrosis factor (TNF) receptor 1 and enhances TNF-induced apoptosis. J. Virol. **72:**3691–3697.